

Supplementary Information

Quantifying cell viability through organelle ratiometric probing

Rui Chen¹, Kangqiang Qiu², Guanqun Han¹, Bidyut Kumar Kundu¹, Guodong Ding¹, Yujie Sun^{1*}, and
Jiajie Diao^{2*}

1. Department of Chemistry, University of Cincinnati, Cincinnati, OH 45221, USA

2. Department of Cancer Biology, College of Medicine, University of Cincinnati, Cincinnati, OH 45267,
USA

* Corresponding authors: Yujie Sun: yujie.sun@uc.edu or Jiajie Diao: jiajie.diao@uc.edu

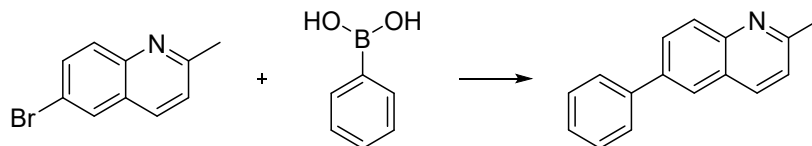
Experimental

Materials. All commercially available chemicals were purchased and used without further treatment, including methanol, ethanol, glycerol, acetone, acetonitrile, chloroform, dimethylformamide (DMF), dimethyl sulfoxide (DMSO), hexane, 6-bromo-2-methylquinoline, phenylboronic acid, methyl iodide, *p*-fluorobenzaldehyde, 1-methylpiperazine. LysoTracker Deep Red (LTDR, #L12492), MitoTracker Red FM (MTR, #M22425), MitoTracker Deep Red FM (MTDR, #M22426), Hoechst 33342 (#H3570), and DAPI were purchased from Invitrogen (Thermo Fisher Scientific). All fluorescent dyes were used according to the product manuals. Carbonyl cyanide *m*-chlorophenylhydrazone (CCCP, #C2759) was purchased from Sigma. Cell Counting Kit-8 (CCK-8) assay was purchased from Dojindo Molecular Technologies. Penicillin, streptomycin, fetal bovine serum (FBS), and Dulbecco's modified Eagle's medium (DMEM) were all purchased from Gibco (Thermo Fisher Scientific). Phosphate-buffered saline (PBS) was purchased from Hyclone (GE Healthcare Life Sciences). Calf thymus DNA solution was purchased from ThermoFisher.

Characterization. The ^1H and ^{13}C NMR spectra were recorded on a Bruker Avance III HD Ascend 400 MHz NMR spectrometer. Chemical shifts for protons are referenced to the residual solvent peak (CDCl_3 , ^1H NMR: 7.26 ppm; D_2O , ^1H NMR: 4.79 ppm; d_6 -DMSO, ^1H NMR: 2.50 ppm), while chemical shifts for carbons are referenced to the residual solvent peaks (CDCl_3 , ^{13}C NMR: 77.16 ppm, d_6 -DMSO; ^{13}C NMR: 39.51 ppm). The following abbreviations (or combinations thereof) were used to explain multiplicities: s = singlet, d = doublet, m = multiplet. Matrix-Assisted Laser Desorption Ionization (MALDI) mass spectrometry was performed on a Bruker Biflex III MALDI-TOFMS instrument.

Synthesis

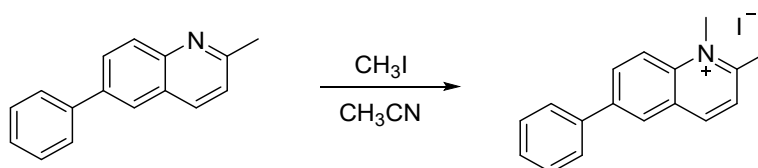
Synthesis of 2-methyl-6-phenylquinoline



To a three-neck round flask, 5.0 mmol (1.11 g) 6-bromo-2-methylquinoline, 1.5 equiv. phenylboronic acid, 0.1 equiv. $\text{Pd}(\text{PPh}_3)_4$, 3.0 equiv. K_2CO_3 , and 0.1 equiv. Bu_4NBr were added under N_2 , then 180 mL toluene, 120 mL EtOH, and 60 mL H_2O were added. The reaction mixture was stirred at 100 °C overnight. When the reaction was finished, the mixture was diluted with EtOAc and washed with water. The

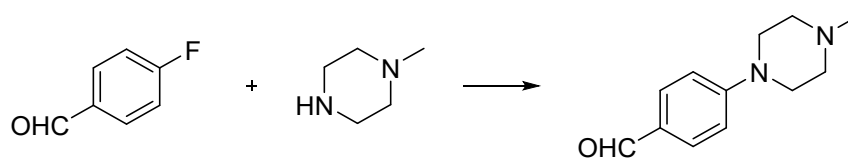
combined organic phase was concentrated. The pure product was obtained through chromatography on silica using EtOAc, EtOH, and hexanes as the eluent. Eventually, 0.72 g target product was obtained with a yield of 65%. ^1H NMR (400 MHz, CDCl_3) δ 8.11-8.08 (m, 2 H), 7.96-7.94 (m, 2 H), 7.73-7.70 (m, 2 H), 7.51-7.47 (m, 2 H), 7.41-7.37 (m, 1 H), 7.32 (d, 1 H), 2.77 (s, 3 H). ^{13}C NMR (100 MHz, CDCl_3) δ 159.16, 147.36, 145.59, 138.58, 136.54, 129.28, 129.15, 129.06, 127.70, 127.51, 126.79, 125.39, 122.56, 25.51.

Synthesis of 1,2-dimethyl-6-phenylquinolin-1-ium



To a 25 mL round flask, 0.5 mmol (110 mg) 2-methyl-6-phenylquinoline and 2.0 equiv. CH_3I were dissolved in 10 mL dry CH_3CN . The reaction mixture was stirred at 80 °C overnight. After being filtered and washed with cool ethanol and dimethyl ether, the pure product was obtained through recrystallization from ethanol. Finally, 40 mg desired product was obtained (yield = 23%). ^1H NMR (400 MHz, DMSO) δ 9.10 (d, 1 H), 8.73 (d, 1 H), 8.66 (d, 1 H), 8.59-8.56 (m, 1 H), 8.13 (d, 1 H), 7.96-7.94 (m, 2 H), 7.60 (m, 2 H), 7.52 (m, 1 H), 4.47 (s, 3 H), 3.08 (s, 3 H). ^{13}C NMR (100 MHz, DMSO) δ 160.86, 145.48, 140.08, 138.63, 137.20, 133.67, 129.41, 129.03, 128.37, 127.35, 127.13, 125.55, 119.79, 22.99.

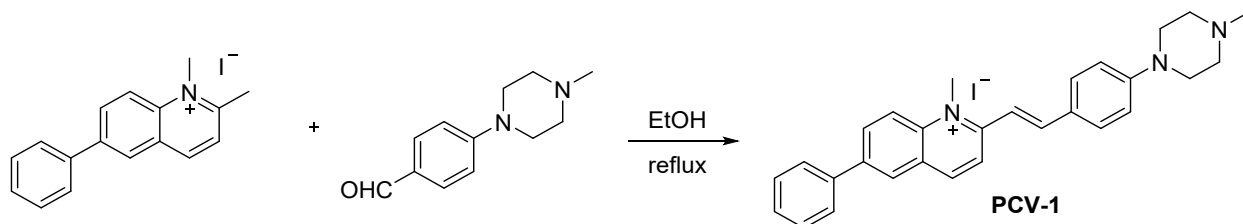
Synthesis of 4-(4-methylpiperazin-1-yl) benzaldehyde



10 mmol *p*-fluorobenzaldehyde (1.24 g), 1.1 equiv. 1-methylpiperazine (1.10 g), 2.0 equiv. K_2CO_3 (2.76 g), and DMF (100 mL) were added to a round flask. The mixture was stirred at 100 °C for 16 h under N_2 . After the reaction was completed, the mixture was poured into cool water and precipitation was formed. The precipitation was filtered and washed with cool water. After drying at room temperature, the pure product was obtained (1.98 g, yield of 97%) through chromatography on silica with EtOAc and hexanes as the eluent. ^1H NMR (400 MHz, CDCl_3) δ 9.76 (s, 1 H), 7.74 (d, 2 H), 6.90 (d, 2 H), 3.40 (t, 4 H), 2.54

(t, 4 H), 2.34 (s, 3 H). ^{13}C NMR (100 MHz, CDCl_3) δ 190.52, 155.11, 131.95, 127.21, 113.64, 54.78, 47.16, 46.22.

Synthesis of 1-methyl-2-(4-(4-methylpiperazin-1-yl)styryl)-6-phenylquinolin-1-ium (PCV-1)



To a round bottom flask, 0.1 mmol 1,2-dimethyl-6-phenylquinolin-1-ium (35.0 mg) and 1.1 equiv. 4-(4-methylpiperazin-1-yl) benzaldehyde (22.4 mg) were dissolved in 10 mL anhydrous ethanol. The solution was refluxed for 48 h under N_2 . After cooling to room temperature, the solvent was evaporated under reduced pressure. The residue was purified by washing with cool ethanol, EtOAc, hexanes, and dimethyl ether. Finally, 25.0 mg desired product was obtained with a yield of 45%. ^1H NMR (400 MHz, DMSO) δ 8.62 (d, 1 H), 8.50 (d, 1 H), 8.19 (s, 2 H), 8.10 (m, 1 H), 8.00 (d, 1 H), 7.85 (d, 2 H), 7.70 (m, 2 H), 7.61 (d, 1 H), 7.52 (m, 2 H), 7.45 (m, 1 H), 4.65 (s, 3 H), 3.35 (m, 4 H), 2.55 (m, 4 H), 2.37 (s, 3 H). ^{13}C NMR (100 MHz, DMSO) δ 148.73, 142.43, 138.63, 137.46, 134.86, 133.84, 132.56, 129.44, 127.57, 127.23, 126.86, 124.68, 122.08, 119.24, 115.45, 113.93, 112.93, 106.55, 94.27, 54.34, 46.62, 41.52, 29.71.

Absorption and emission measurements. PCV-1 in aqueous solution (10 μM) was transferred to a quartz cuvette with 1 cm optical length to measure the absorption spectra on an Agilent Cary 8453 spectrophotometer. The fluorescence spectra were recorded on a HORIBA Fluorolog QM spectrofluorometer.

The measurements of lipophilicity. Lipophilicity was determined by a shake-flask ultraviolet spectrophotometry method to measure the *n*-octanol/water partition coefficients (logP).¹ First, 25 mL 1-octanol and 25 mL aqueous buffer solution were mixed at room temperature. After 24 h, the standard solutions of the sample (10 μM) were prepared by using the preceding saturated 1-octanol phase and aqueous buffer phase solution, respectively. Next, the test solutions were prepared by mixing 10 ml standard solution in 1-octanol and 10 ml standard solution in aqueous buffer solution. After shaking, the mixture of test solution was centrifuged for 5 min. The 1-octanol phase layer was separated from the water phase layer and the absorbance of the two layers was measured on an Agilent Cary 8453

spectrophotometer. Based on the Beer-Lambert law, the concentrations of the sample in the 1-octanol phase (C_o) and the aqueous phase (C_w) were calculated. Finally, the n-octanol/water partition coefficients ($\log P$) were further calculated by using the following equation.

$$\log P = \log (C_o/C_w)$$

Förster–Hoffmann equation. The linear relationship between $\log I_{605\text{ nm}}$ and $\log \eta$. Förster–Hoffmann equation: $\log I = x \log \eta + C$, where I is the emission intensity, x is the sensitivity of the probe towards viscosity, η is the viscosity, and C is a constant.^{2,3}

Photostability test. The photostability test of probes was investigated under a light irradiation wavelength of 488 nm for 300 s.

Phosphate buffer solution. A series of standard pH buffer solutions were prepared by mixing 0.2 M KH_2PO_4 , 0.2 M $\text{Na}_2\text{HPO}_4 \cdot 7\text{H}_2\text{O}$, and 0.2 M H_3PO_4 with different volume ratios, and the pH values were measured using a Mettler Toledo pH-meter.

Computational methods of DFT. All calculations were performed with the Gaussian 16W program package employing the DFT method with Becke's three-parameter hybrid functional and Lee-Yang-Parr's gradient corrected correlation functional (B3LYP).^{4,6} 6-31G* basis set was applied for H, C, and N.⁷ The geometries of the singlet ground states of compounds were optimized in H_2O using the conductive polarizable continuum model (CPCM). The local minimum on each potential energy surface was confirmed by frequency analysis. Time-dependent DFT calculations produced the singlet excited states of each compound starting from the optimized geometry of the corresponding singlet ground state, using the CPCM method with H_2O as the solvent. The calculated absorption spectra, electronic transition contributions, and electron density difference maps (EDDMs) were generated by GaussSum 3.0.⁸ The electronic orbitals were visualized using VMD 1.9.4. Isovalue was 0.04 for plotting HOMOs, LUMOs, and EDMs.⁹

Molecular docking calculations. The molecular docking calculations were performed using the AutoDock Vina software.¹⁰ The structure of PCV-1 was obtained from previous DFT calculations via

Gaussian 16W software. The initial structures of DNA were downloaded from the protein data bank (PDB ID: 1D30).¹¹

Cell culture. HeLa cells were gifted from Dr. Carolyn M. Price lab (University of Cincinnati). Cells were cultured in DMEM containing 10% FBS, 100 units mL⁻¹ streptomycin, and 100 units mL⁻¹ penicillin. The cells were cultured in the incubator (Thermo Fisher Scientific) at 37°C with 5% CO₂ and 100% humidity.

Structured illumination microscopy (SIM). Super-resolution images were performed on a commercial Nikon Structured Illumination Microscopy (N-SIM, version AR5.11.00 64 bit, Tokyo, Japan) super-resolution microscope. Images were obtained at 512 × 512 by using the Nikon NIS-Elements software, and the raw images were reconstructed and analyzed with Nikon NIS-Elements and ImageJ. Cells were cultured on a 35 × 10 mm dish for 24 h for imaging. Cells were seeded on culture dishes for 24 h to adhere. The colocalization experiments were obtained with a dual-channel imaging mode. HeLa cells were stained by PCV-1 (0.4 μM, 30 min). The Pearson's colocalization coefficient (PCC) values were analyzed and calculated using the CellProfiler software. Quantification of fluorescence intensity ratios was collected via ImageJ and Excel.

Cell viability and cytotoxicity assay (CCK-8): HeLa cells were seeded in a 96-well plate with a density of 1 × 10⁴ cells/well in 100 μL culture medium. After 24 h to adhere, different concentrations of PCV-1 were added to the well plate and incubated for 24 h. Next, 10 μL CCK-8 was added to each cell well plate for incubating for 1 h. Next, the absorbance at 490 nm was obtained using a microplate reader (BioTek Instruments, Inc., USA). The viability of CCCP-treat cells were also measured with the same method.

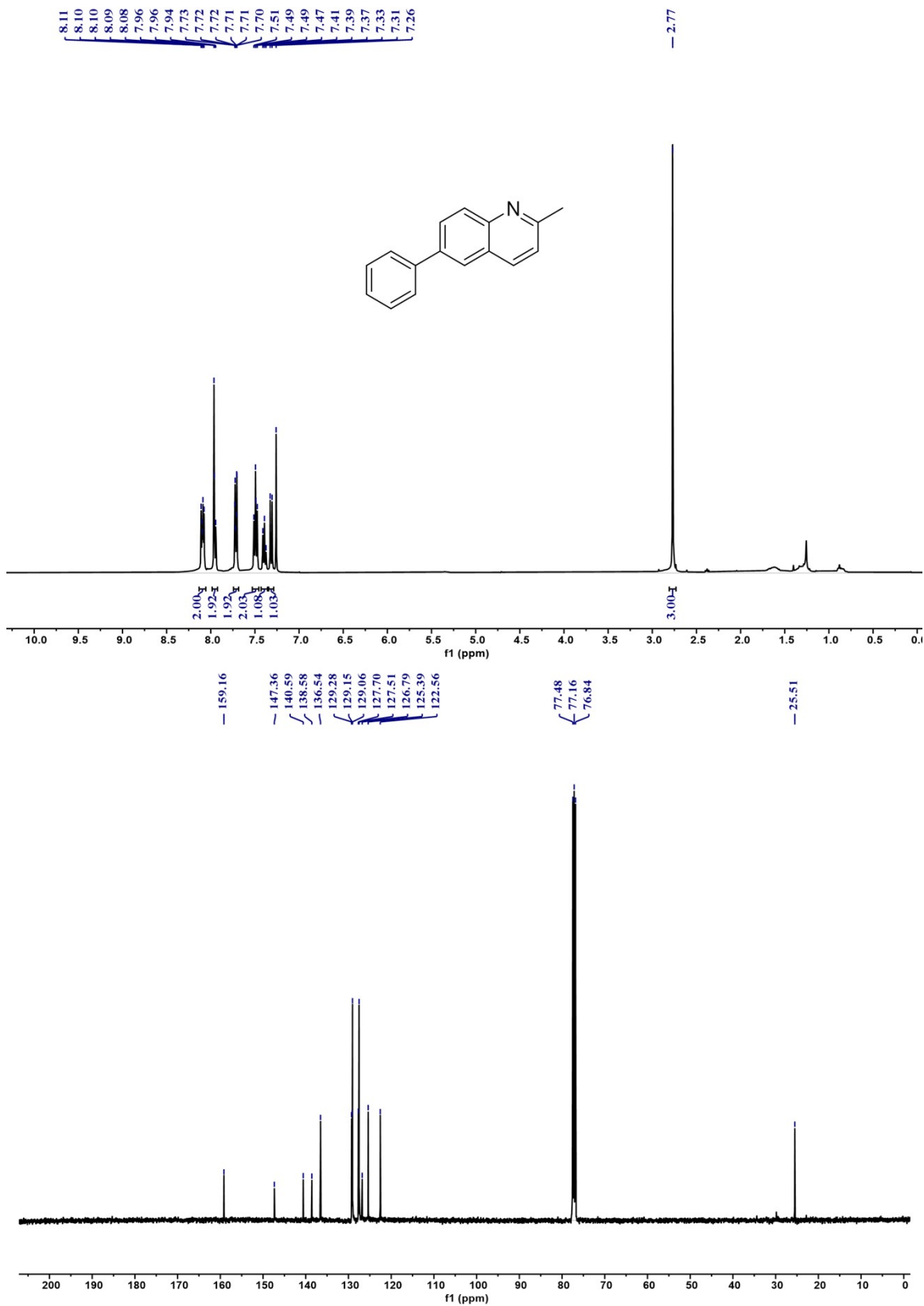


Fig. S1 ¹H NMR (top) and ¹³C NMR (below) spectra of 2-methyl-6-phenylquinoline.

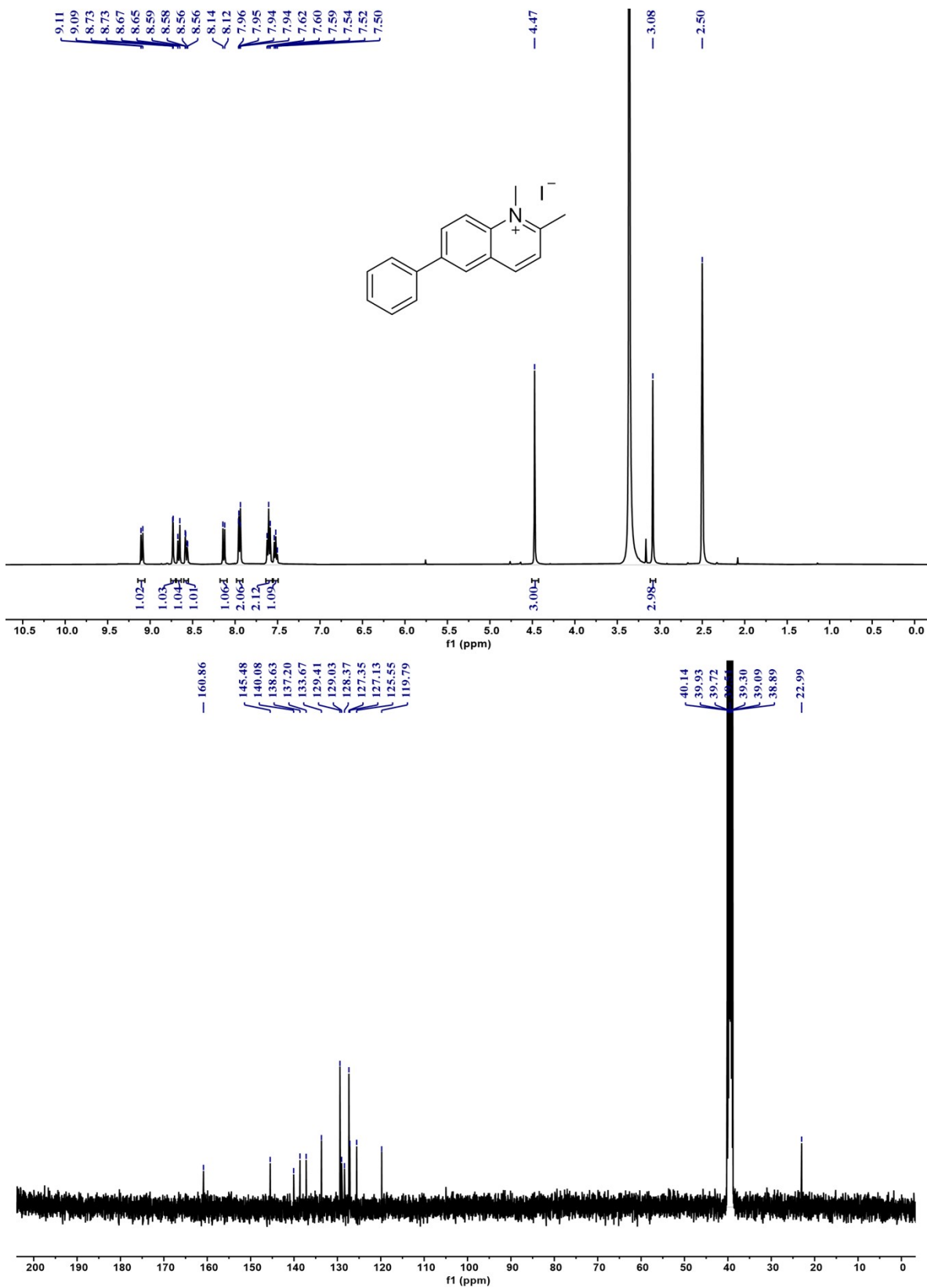


Fig. S2 ^1H NMR (top) and ^{13}C NMR (below) spectra of 1,2-dimethyl-6-phenylquinolin-1-ium.

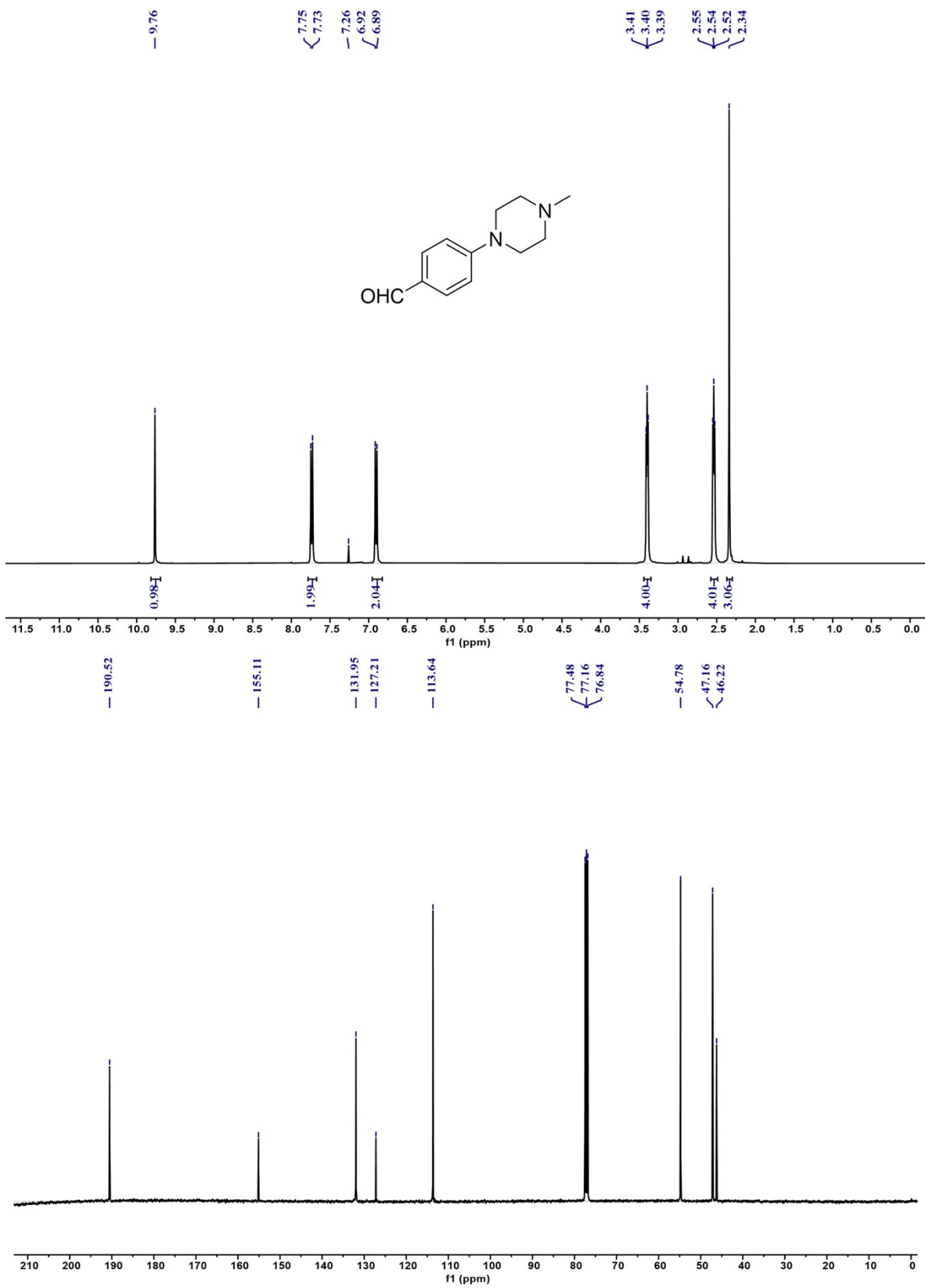


Fig. S3 ¹H NMR (top) and ¹³C NMR (below) spectra of 4-(4-methylpiperazin-1-yl) benzaldehyde.

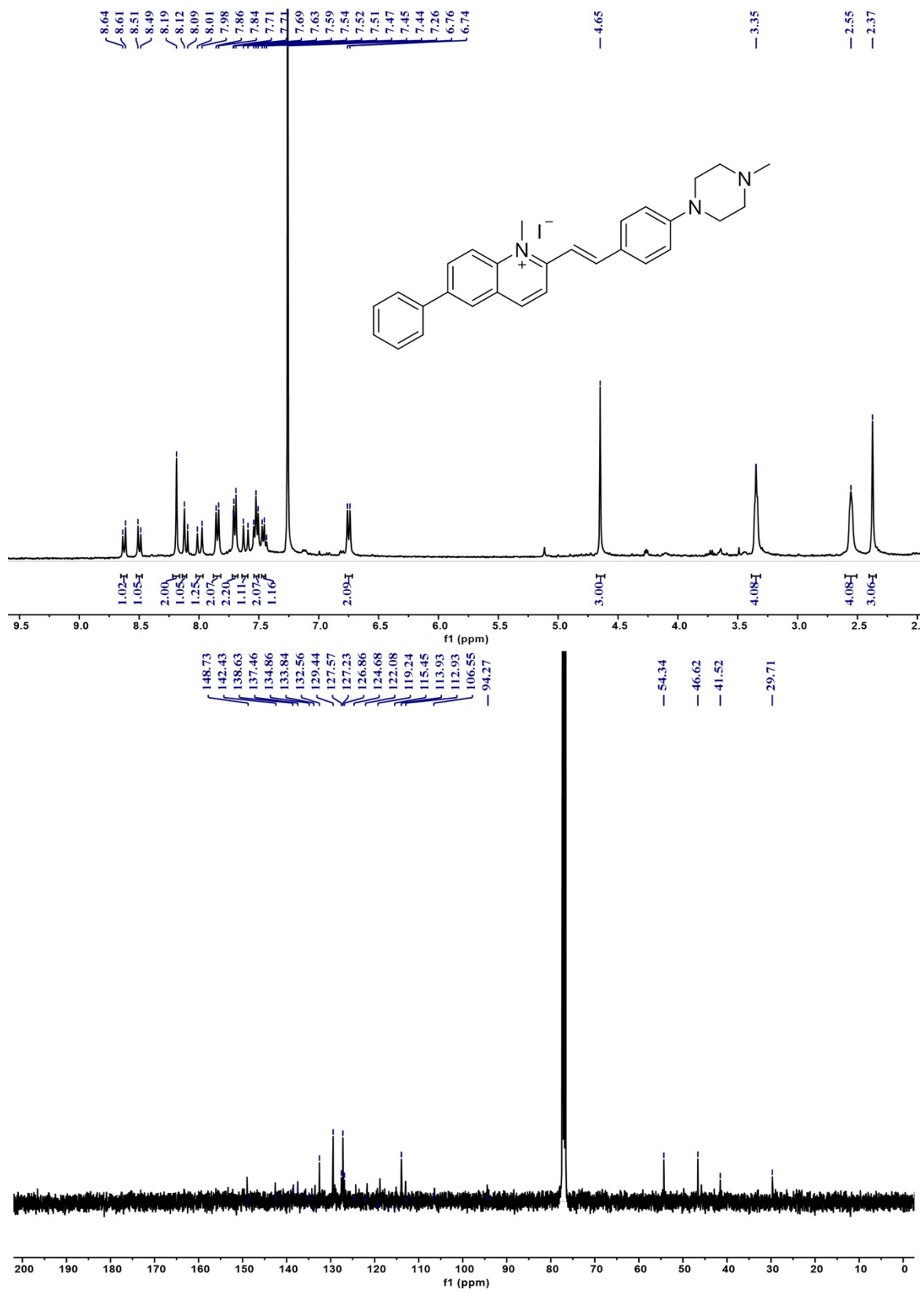


Fig. S4 ¹H NMR (top) and ¹³C NMR (below) spectra of PCV-1.

Sample ID: [Sample 2] (C₂₉H₃₀N₃)⁺ 547 Da (in DMSO/MeOH)

TOF MS ES+
7.14e12

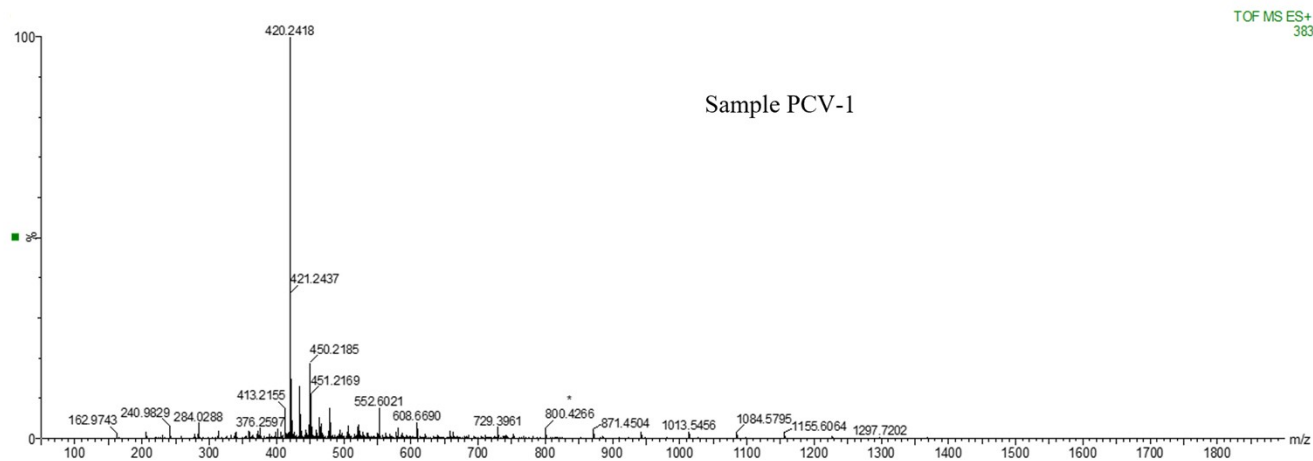
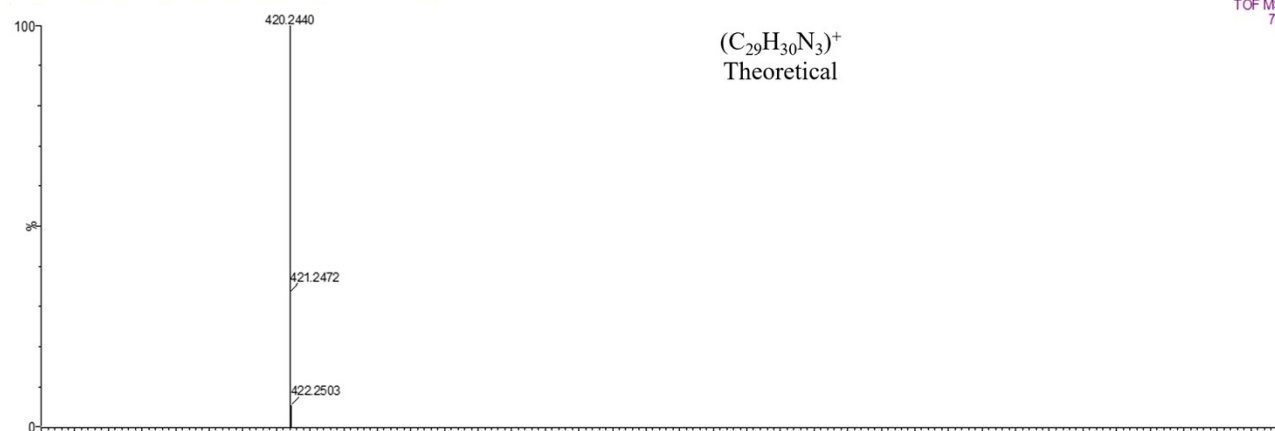


Fig. S5 Mass spectra of PCV-1.

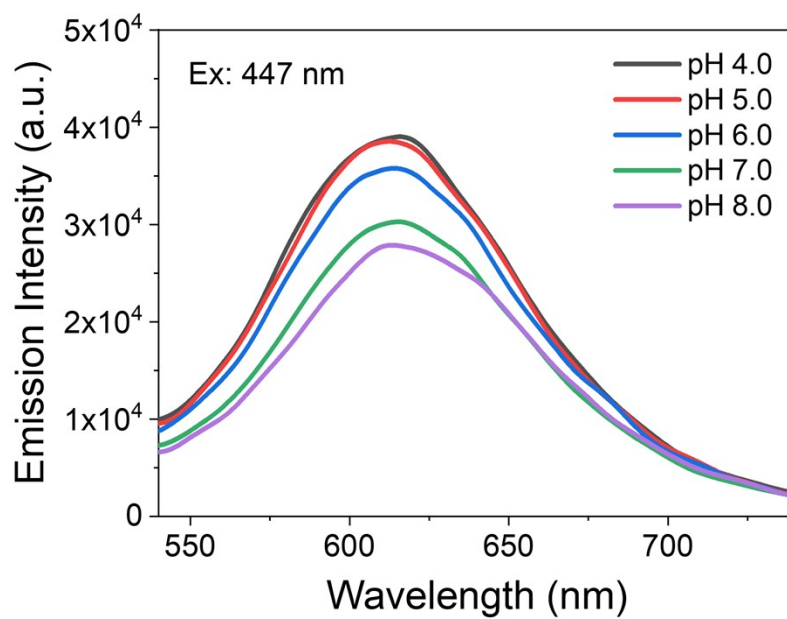


Fig. S6 Emission spectra of PCV-1 in buffer solutions with different pH values.

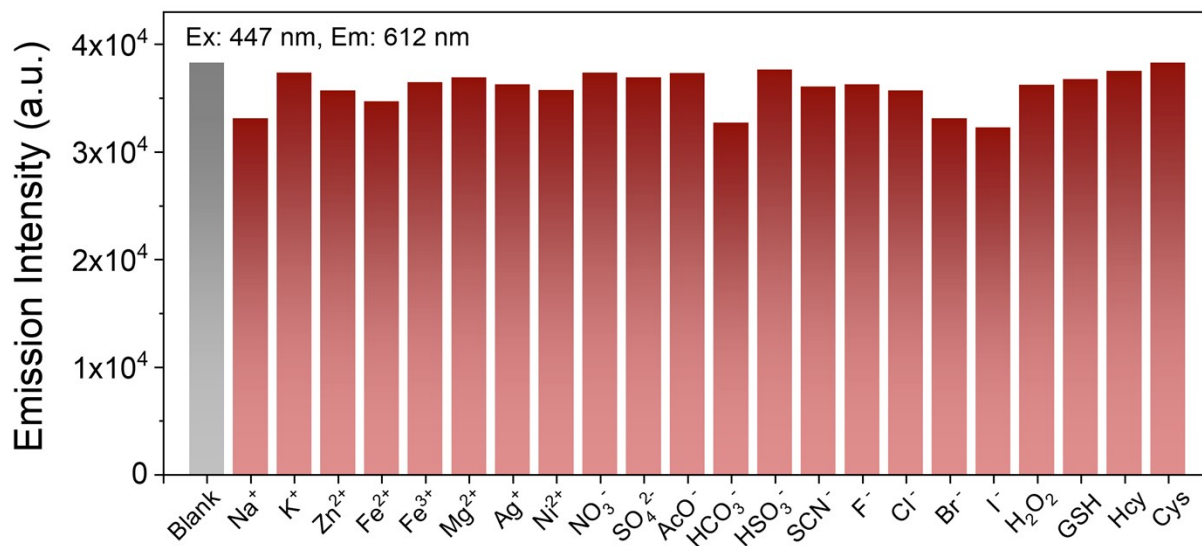


Fig. S7 Emission intensity histogram plots of PCV-1 in aqueous solution with additional chemical species. Conditions: the concentration of Na⁺ to H₂O₂ is 100 μM, and the concentration of GSH to Cys is 200 μM.

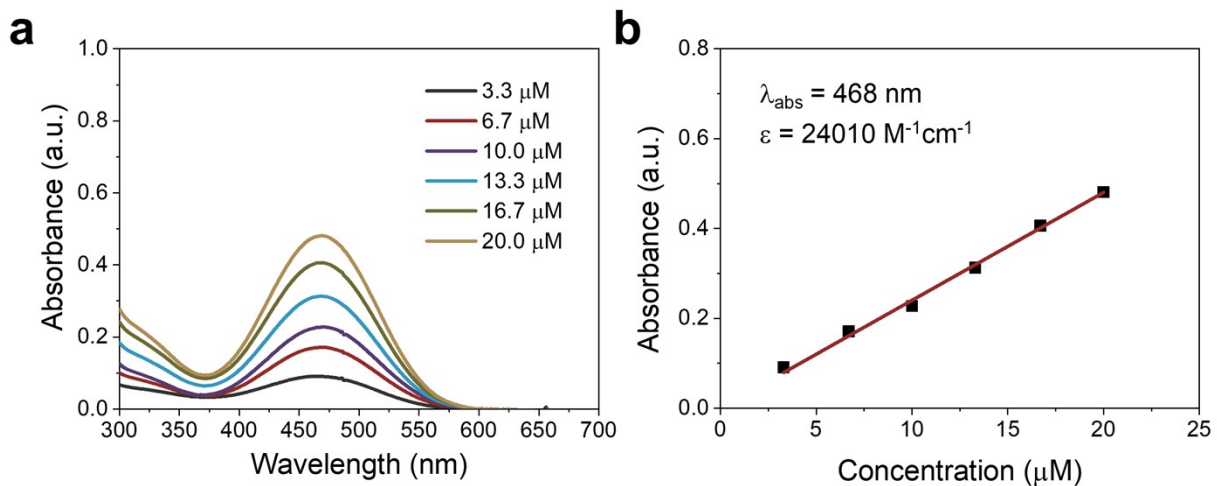


Fig. S8 (a) Absorption spectra of different concentrations of PCV-1 in high viscosity solution ($\eta = 49 \text{ cP}$). (b) Linear plot of absorbance at 468 nm versus different concentrations of PCV-1 in high viscosity solution ($\eta = 49 \text{ cP}$).

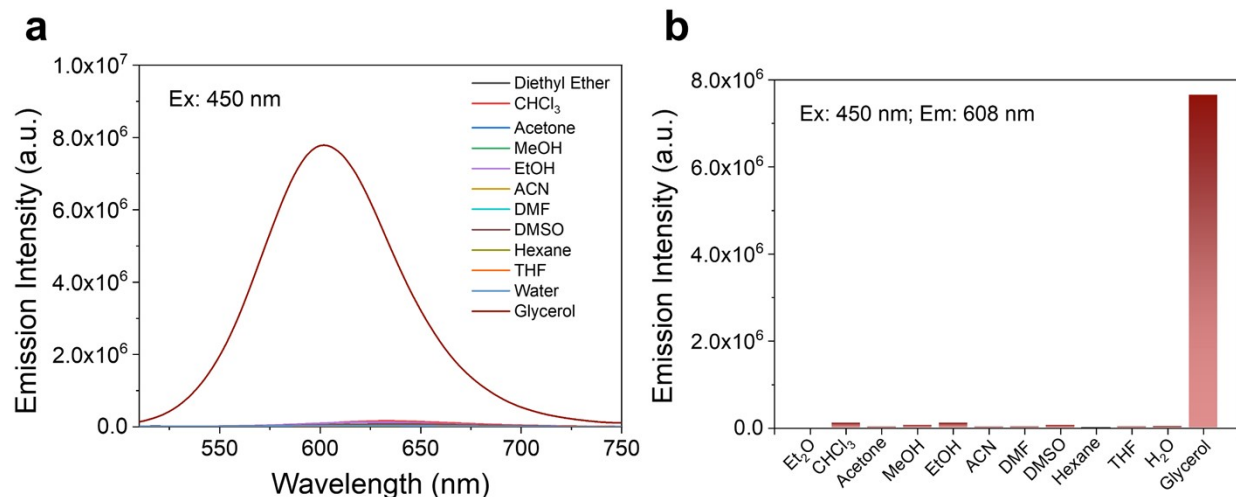


Fig. S9 (a) Emission spectra of PCV-1 in different solvents. (b) Emission intensity histogram plots of PCV-1 in different solvents.

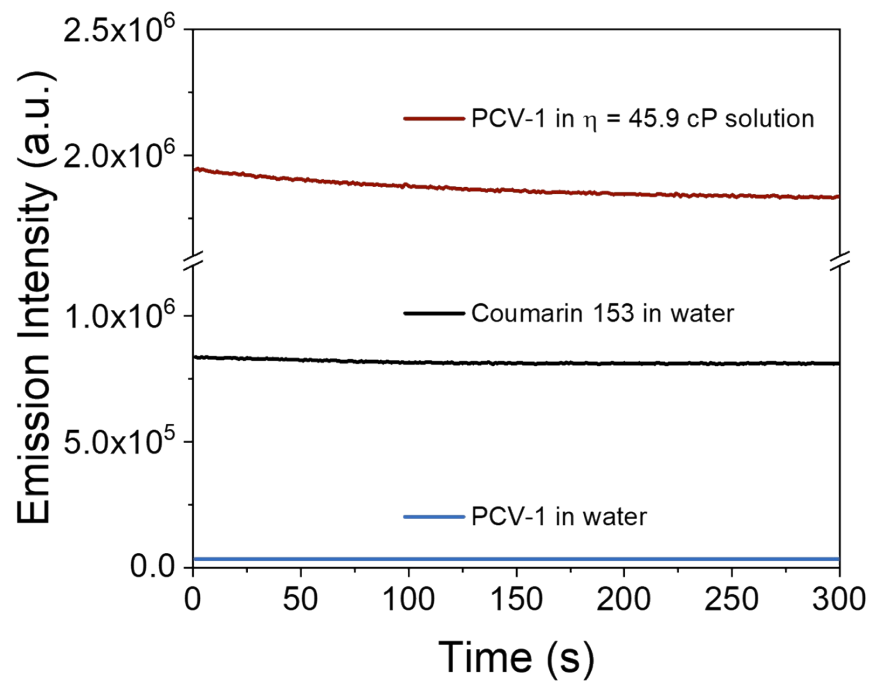


Fig. S10 The photostability tests of PCV-1 in water and high viscosity (49 cP) solutions, $\lambda_{ex} = 488$ nm, $\lambda_{em} = 610$ nm. The photostability test of coumarin 153 in water, $\lambda_{ex} = 488$ nm, $\lambda_{em} = 550$ nm.

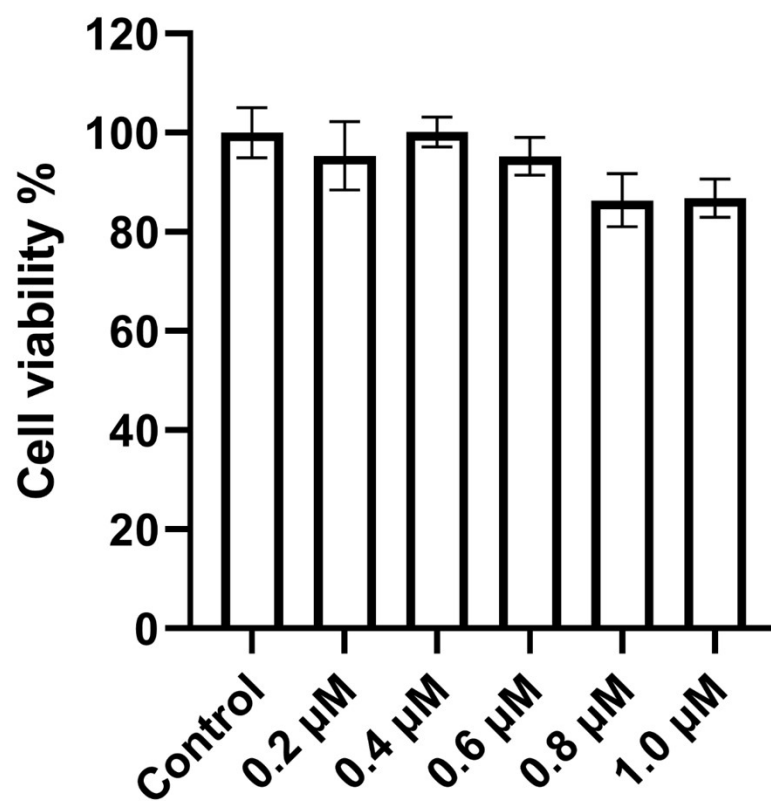


Fig. S11 Cell viability test after HeLa cells were treated with different concentrations of PCV-1 for 24 hours.

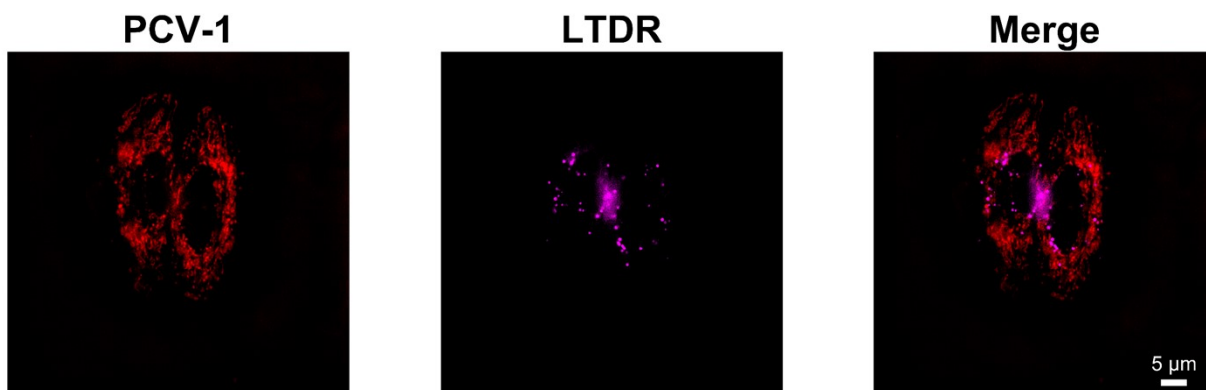


Fig. S12 SIM images of HeLa cells co-stained with PCV-1 and LTDR.

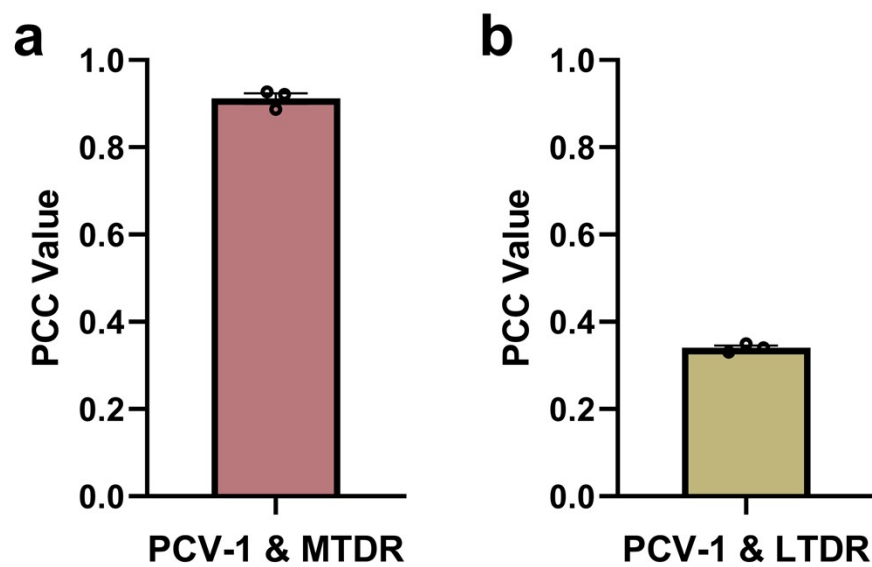


Fig. S13 (a) PCC values of PCV-1 with MTDR. (b) PCC values of PVC-1 with LTDR. Data are given as $M \pm SEM$, $n = 3$.

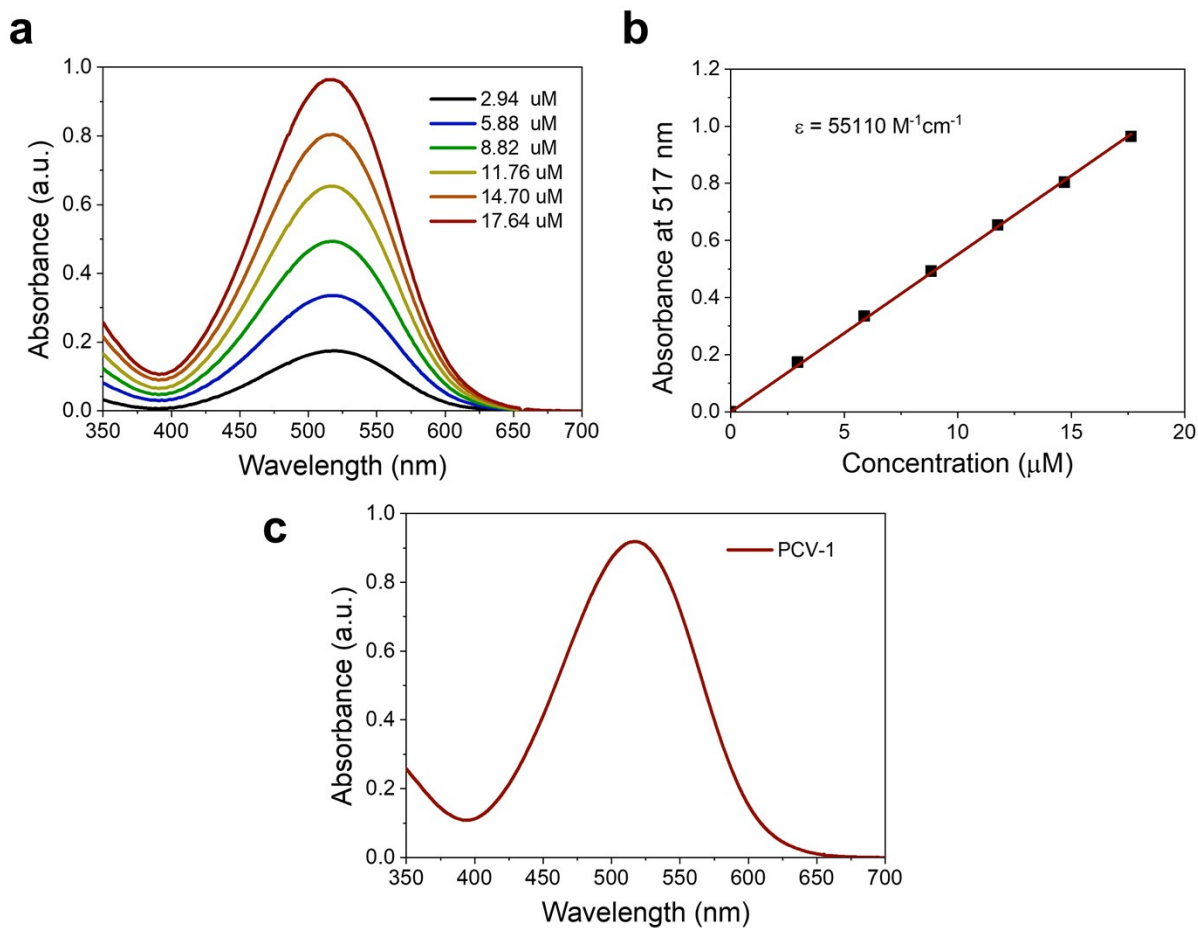


Fig. S14 The measurement of lipophilicity (partition coefficient). (a) Absorption spectra of different concentrations of PCV-1 in PBS buffer solution containing saturated 1-octanol. (b) Scatter plots and linear relationship between absorbance at 517 nm and concentrations of PCV-1. (c) Absorption spectrum of PCV-1 in PBS buffer solution containing saturated 1-octanol after phase separation.

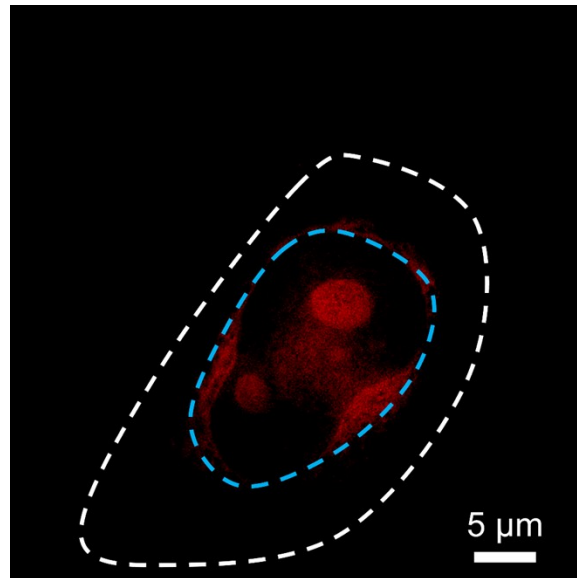


Fig. S15 SIM images of dead HeLa cells stained with PCV-1.

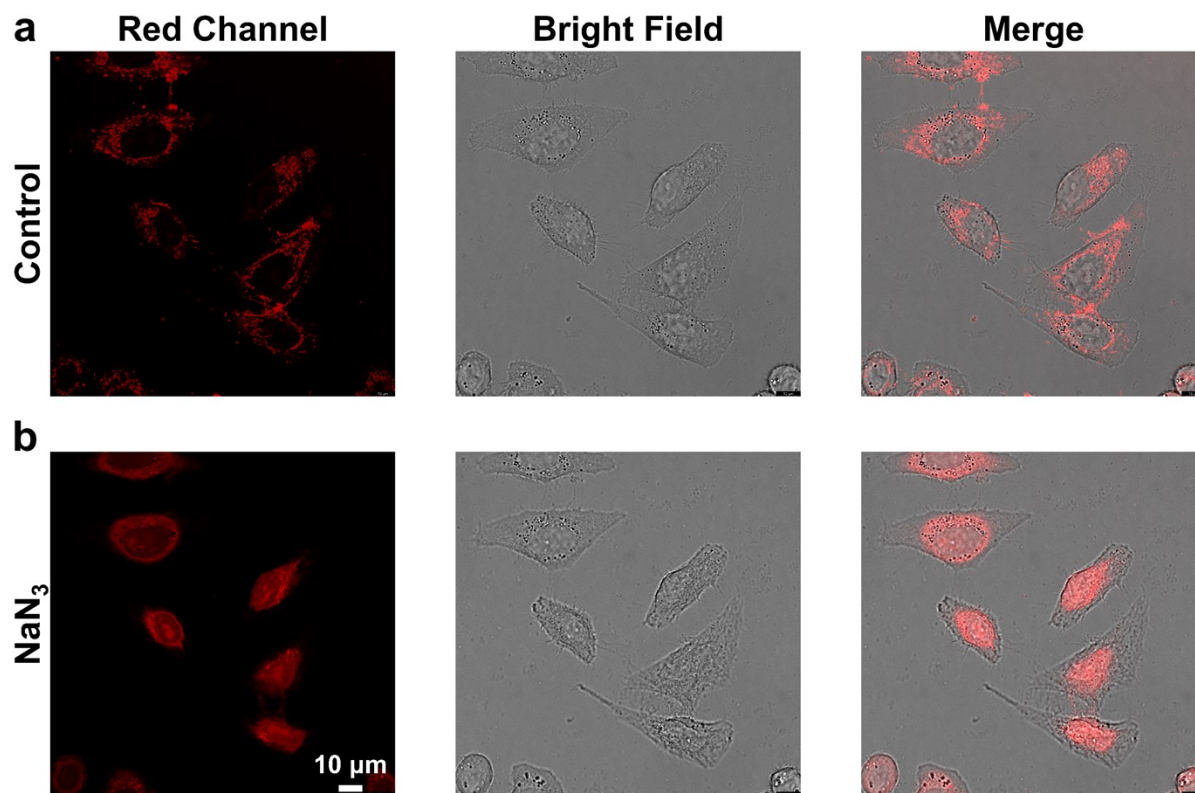


Fig. S16 (a) Confocal images of HeLa cells stained with PCV-1. (b) Confocal images of PCV-1-stained HeLa cells treated with NaN₃. NaN₃ treatment condition: 5% NaN₃ for 10 min. High-resolution confocal images were acquired on a commercial Leica Stellaris 8 confocal microscope under LIGHTNING mode.

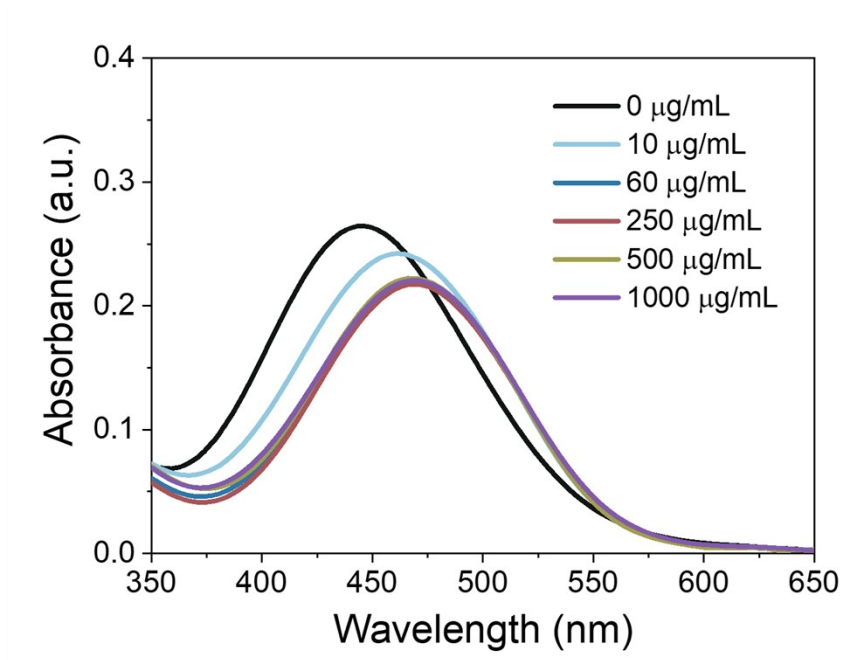


Fig. S17 Absorption spectra of PVC-1 in buffer solutions with adding different concentrations of calf thymus DNA.

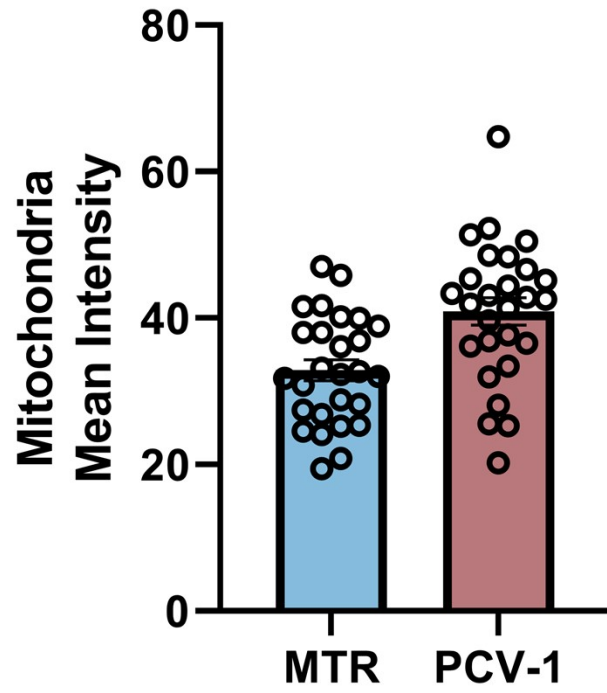


Fig. S18 Mitochondria mean intensity of MTR and PCV-1. Data are given as $M \pm SEM$, $n = 27$.

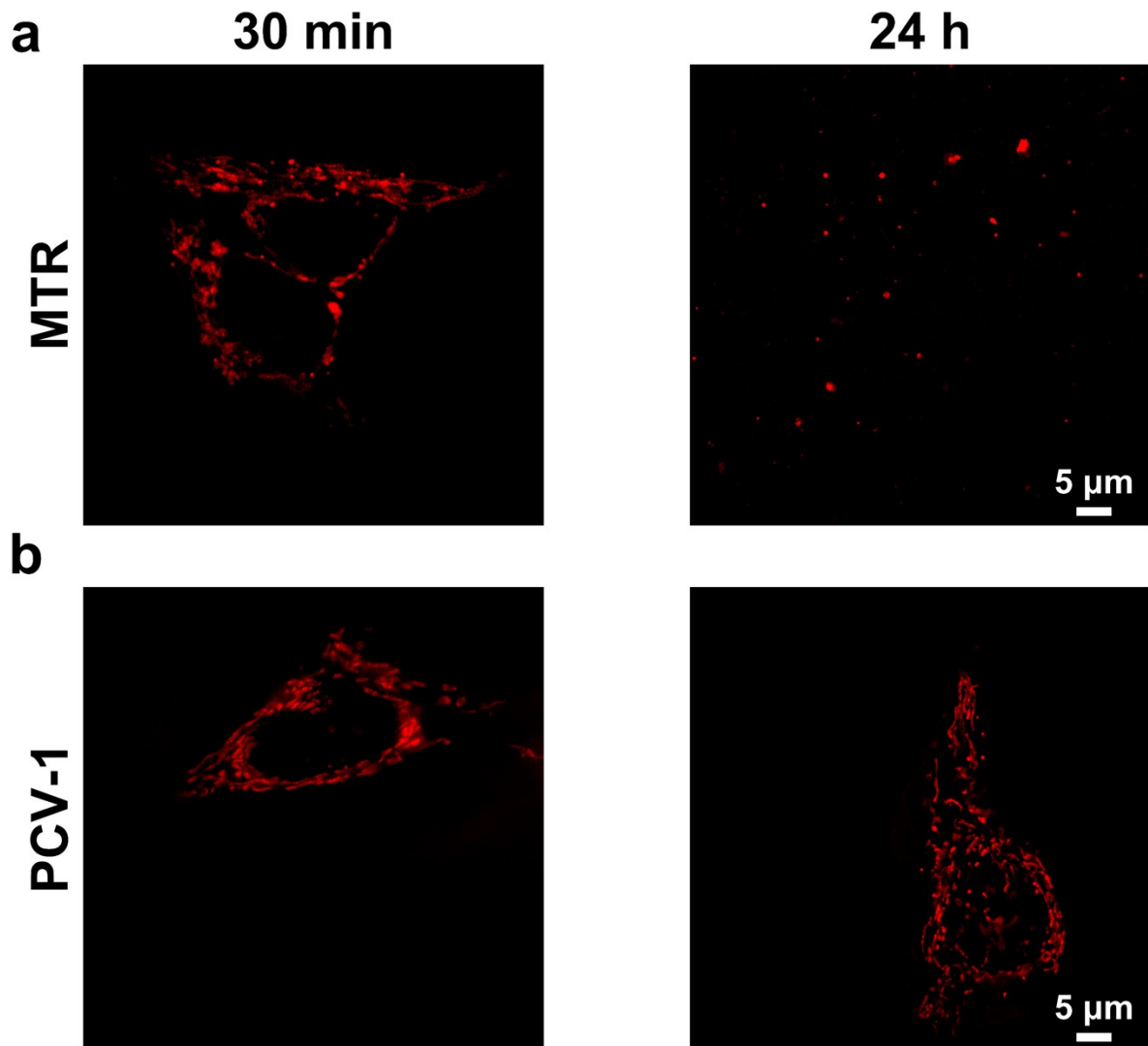


Fig. S19 (a) SIM images of HeLa cells stained with MTR for 30 min and 24 h. (b) SIM images of HeLa cells stained with PCV-1 for 30 min and 24 h.

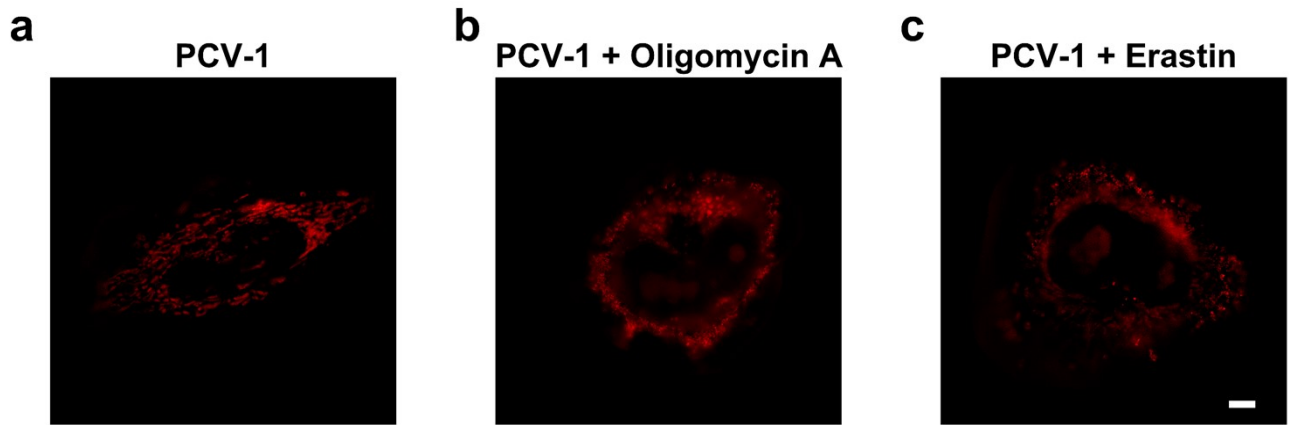


Fig. S20 (a) SIM images of HeLa cells stained with PCV-1. SIM images of HeLa cells stained with PCV-1 after treatment of (b) 40 μ M oligomycin A for 4 h, (c) 40 μ M erastin for 4 h. Scale bars: 5 μ m.

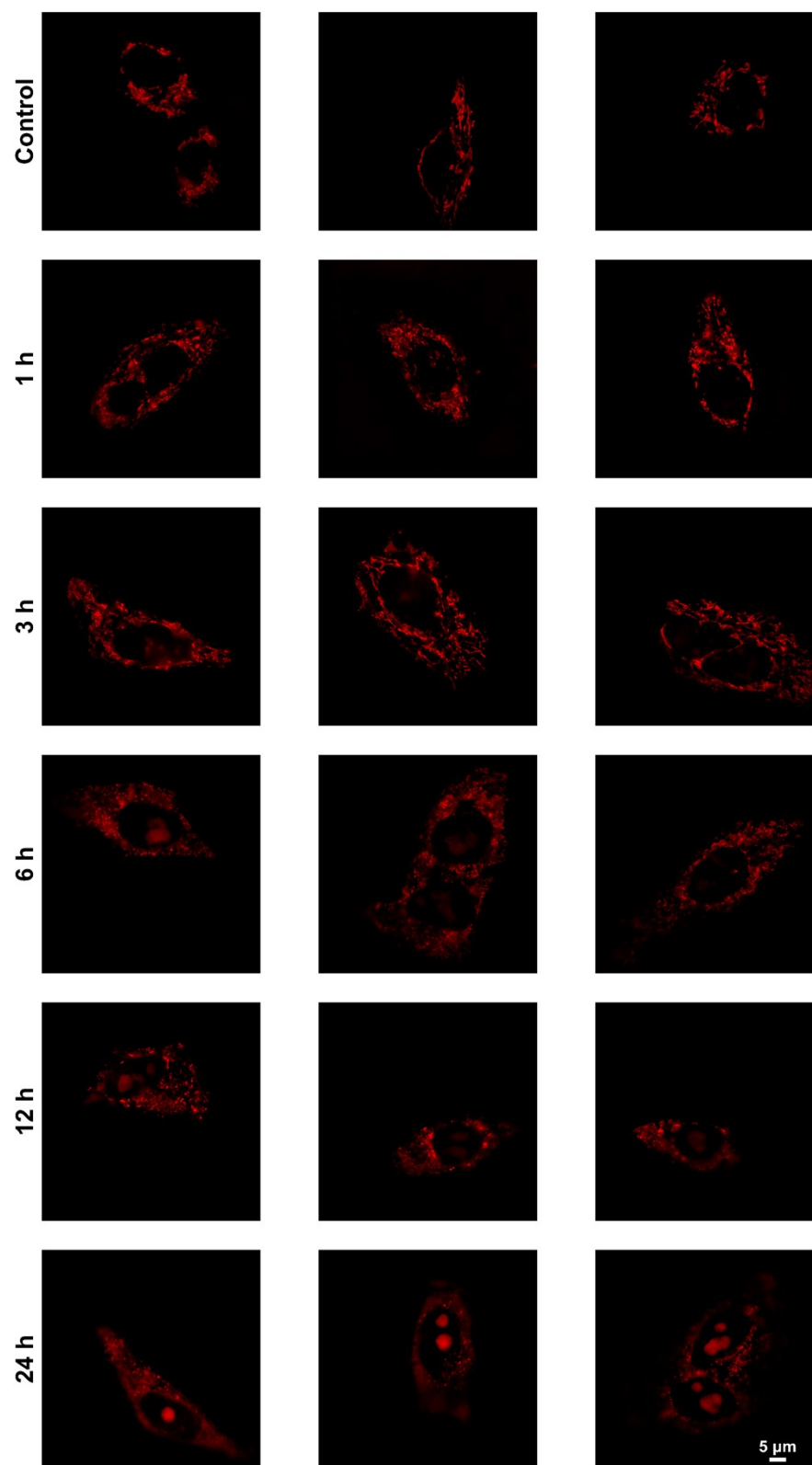


Fig. S21 The data set for **Fig. 6d**.

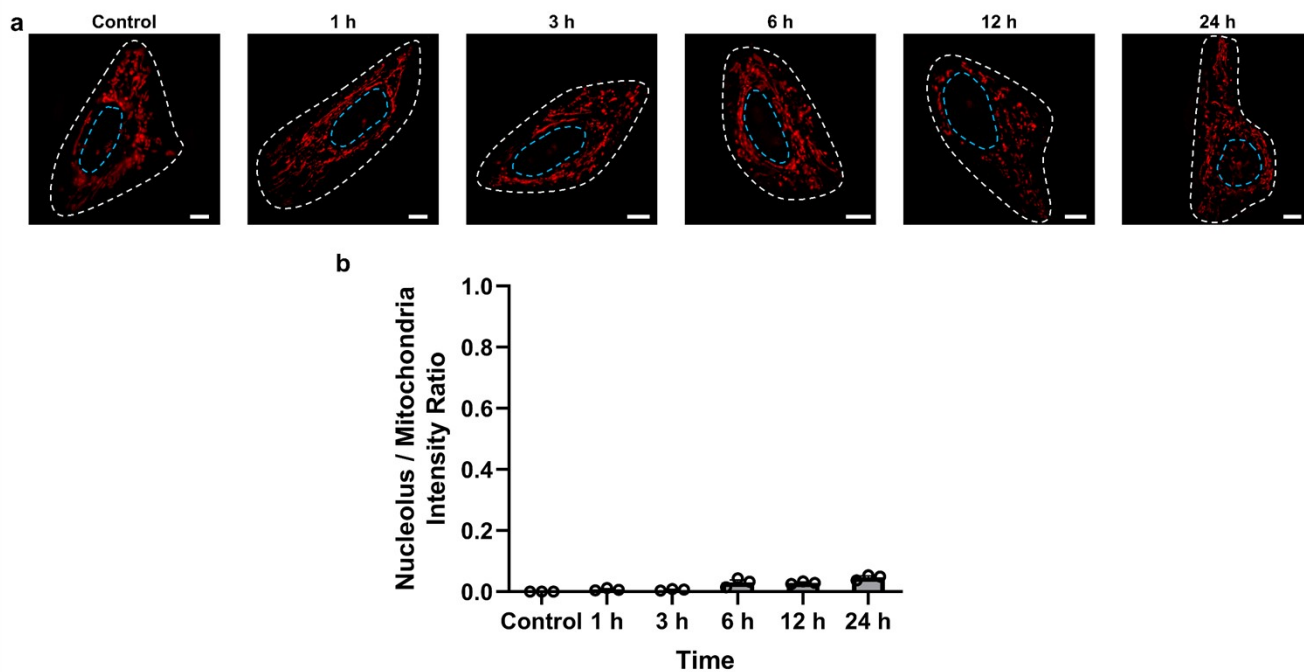


Fig. S22 (a) SIM images of HeLa cells stained with PCV-1 at different times (0-24 h). PCV-1 channel: Ex 561 nm, Em 570-640 nm; scale bars: 5 μ m. (b) The fluorescence intensity ratio of nucleolus to mitochondria in PCV-1-stained HeLa cells at different times (0-24 h). Data are given as $M \pm SEM$, $n = 3$.

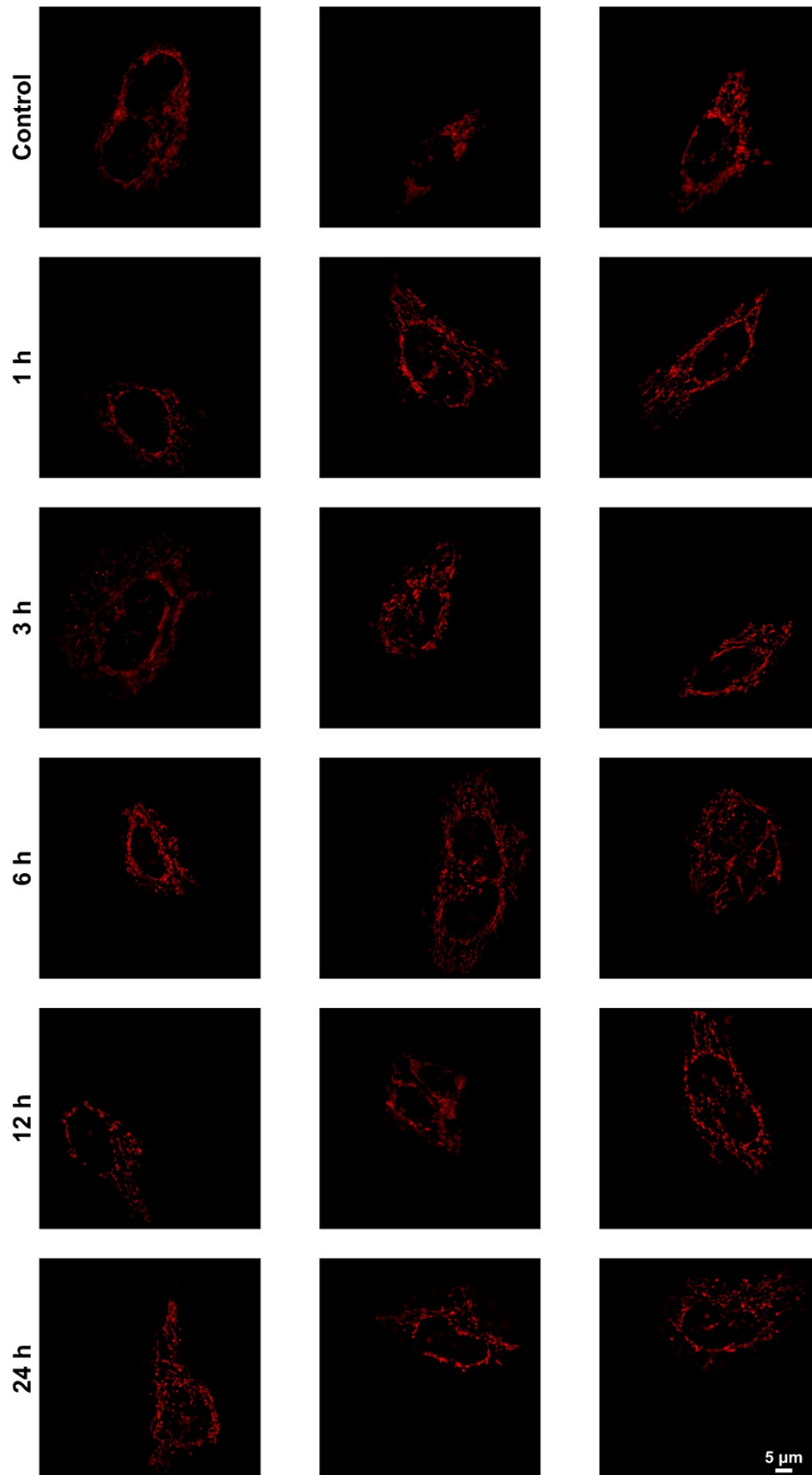


Fig. S23 The data set for **Fig. S22b**.

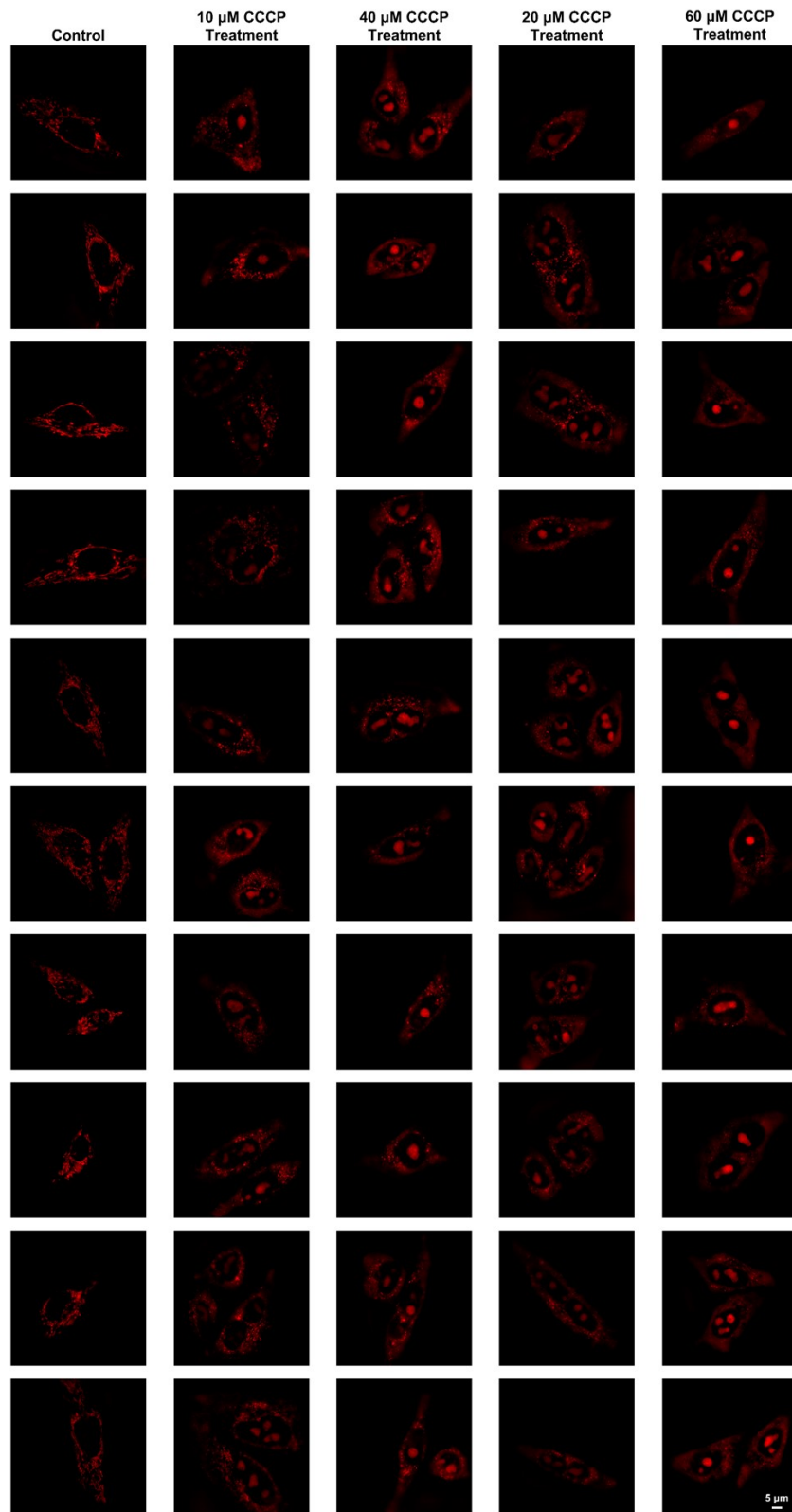


Fig. S24 The data set for **Fig. 7c**.

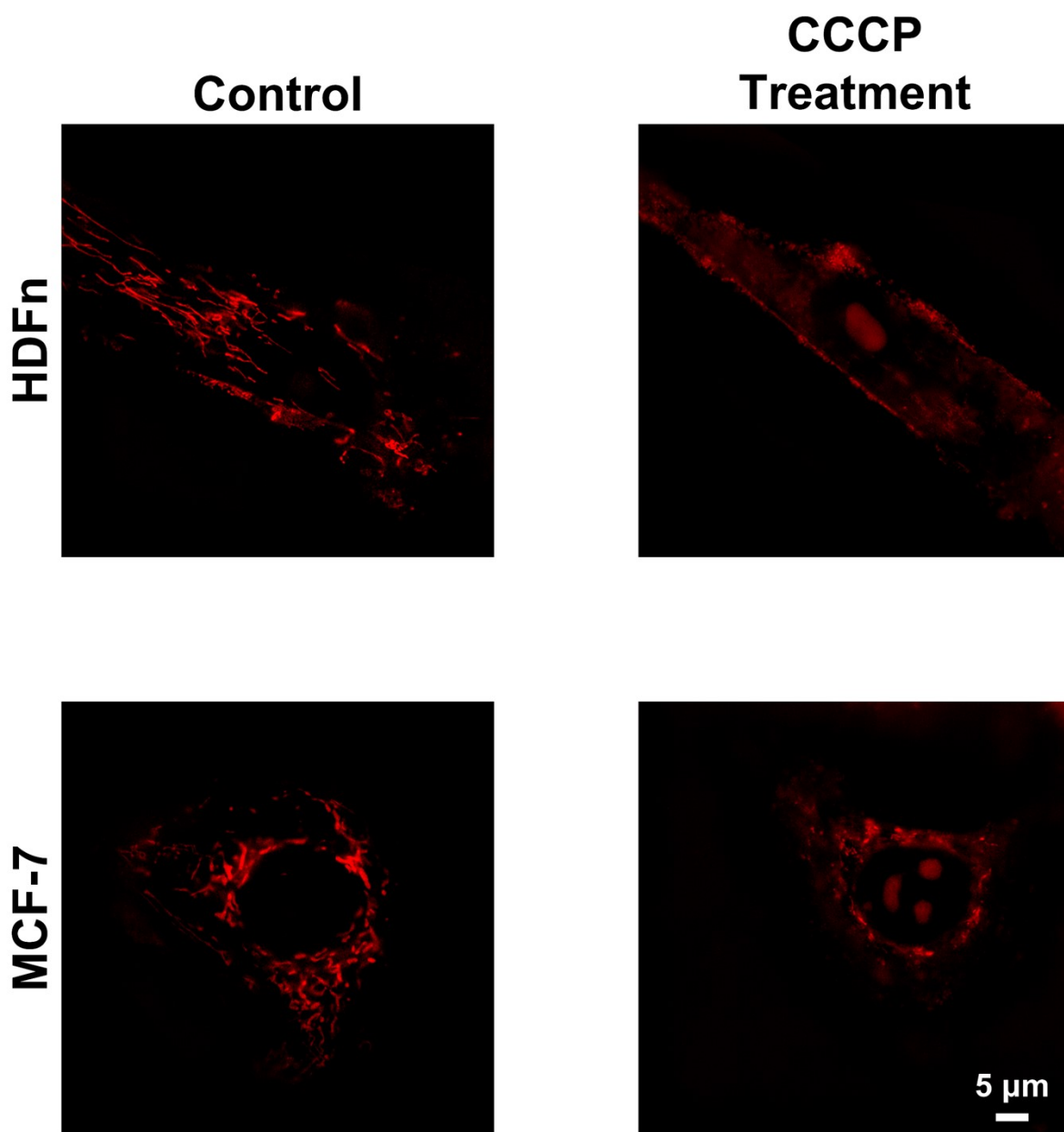


Fig. S25 SIM images of HDFn and MCF-7 cells treated with/without CCCP. CCCP treatment condition: 20 μ M CCCP for 24 h.

Table S1 Calculated molecular orbitals of PCV-1 in H₂O.

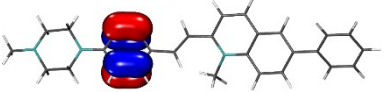
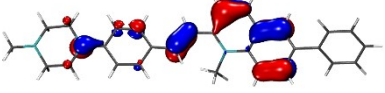
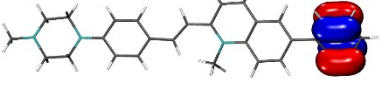
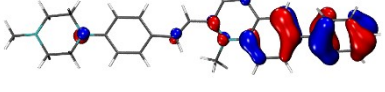
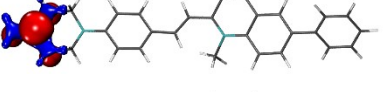
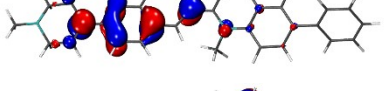
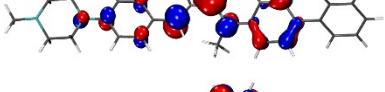

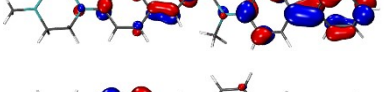
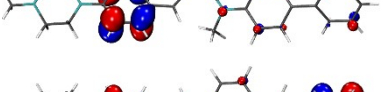
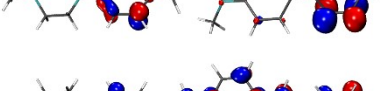
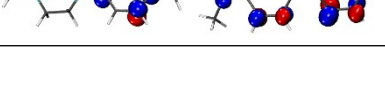
MOs	Energy (eV)	Orbitals
HOMO-5 (107)	-7.256	
HOMO-4 (108)	-7.113	
HOMO-3 (109)	-7.039	
HOMO-2 (110)	-6.509	
HOMO-1 (111)	-6.086	
HOMO (112)	-5.473	
LUMO (113)	-2.947	
LUMO+1 (114)	-1.612	
LUMO+2 (115)	-1.086	
LUMO+3 (116)	-0.343	
LUMO+4 (117)	-0.278	
LUMO+5 (118)	-0.182	

Table S2 Calculated singlet electron transitions ($f > 0.01$) of PCV-1 in H₂O.

No.	Wavelength (nm)	f	Major contributions
1	533.4	1.4467	HOMO->LUMO (100%)
2	439.7	0.0186	H-1->LUMO (100%)
3	395.0	0.0573	H-2->LUMO (94%)
4	357.1	0.3432	HOMO->L+1 (94%)
5	338.0	0.0697	H-4->LUMO (26%), H-3->LUMO (66%)
6	335.7	0.0707	H-4->LUMO (59%), H-3->LUMO (33%)
8	307.0	0.0667	H-6->LUMO (57%), HOMO->L+2 (33%)
9	302.1	0.0157	H-6->LUMO (35%), HOMO->L+2 (50%)
10	294.8	0.0102	H-1->L+1 (98%)
11	280.1	0.3563	H-2->L+1 (73%)
12	276.0	0.0314	HOMO->L+3 (72%), HOMO->L+4 (11%)
15	256.9	0.0111	H-3->L+1 (36%), HOMO->L+4 (39%)
16	254.5	0.0123	H-3->L+1 (26%), HOMO->L+4 (14%), HOMO->L+5 (38%)
18	247.4	0.1342	H-4->L+1 (10%), H-2->L+2 (82%)
19	239.0	0.1413	H-6->L+1 (10%), H-5->L+1 (10%), H-4->L+1 (52%)
20	237.3	0.0435	H-5->L+1 (57%), H-1->L+3 (22%)
21	236.2	0.0199	H-3->L+1 (11%), H-3->L+2 (43%), H-2->L+4 (15%)
22	235.5	0.0485	H-6->L+1 (11%), H-1->L+3 (32%), HOMO->L+6 (24%)
23	235.2	0.0418	H-6->L+1 (21%), H-5->L+1 (18%), H-1->L+3 (27%), HOMO->L+6 (19%)
24	230.5	0.1628	H-6->L+1 (31%), HOMO->L+6 (42%)
26	223.6	0.0142	H-9->LUMO (11%), H-4->L+2 (30%), H-1->L+4 (15%), H-1->L+5 (11%)
27	223.2	0.0497	H-10->LUMO (31%), H-8->LUMO (41%)
28	222.4	0.0787	H-9->LUMO (57%), H-4->L+2 (12%)
29	219.4	0.0212	H-10->LUMO (48%), H-8->LUMO (38%)

Cartesian coordinates of optimized PCV-1

Charge = +1, Multiplicity = 1

C	8.31137100	-0.80448500	-1.01450200
C	9.69361800	-0.83946300	-1.18530500
C	10.50622900	0.08313400	-0.52332800
C	9.92748900	1.04275900	0.30940000
C	8.54491700	1.08099300	0.47874600
C	7.71605700	0.15604100	-0.17896100
C	6.24659400	0.19250600	0.00710100
C	5.48229700	-0.96859700	0.04401200
C	4.08361400	-0.93547700	0.21366200
C	3.42086200	0.31324300	0.36993200
C	4.18851700	1.49353800	0.32362400
C	5.55850200	1.42400500	0.14312900
C	3.29609200	-2.12076500	0.25028400
C	1.93905800	-2.04225900	0.35865800
C	1.26406200	-0.78923600	0.46086800
N	2.03362400	0.34281100	0.56530400
C	-0.16855700	-0.80896600	0.44442700
C	-1.03541300	0.16138800	-0.00173600
C	-2.45999400	0.07583300	-0.08639600
C	-3.18230200	1.13405500	-0.69056600
C	-4.55474400	1.11867700	-0.80898700
C	-5.32532700	0.02432900	-0.31880200
C	-4.59724100	-1.04661200	0.28746500
C	-3.22785100	-1.01425200	0.40037200
N	-6.69040300	0.00779200	-0.40015900
C	-7.46583300	1.15438600	-0.88897200
C	-8.78438700	1.28587800	-0.12025600
N	-9.55725100	0.05377200	-0.18746600
C	-8.79070000	-1.04162800	0.39101000
C	-7.48319800	-1.23065300	-0.37668600
C	-10.87215200	0.19449400	0.42728900
C	1.44753500	1.61170800	1.03474100
H	7.68704200	-1.50718100	-1.55951000
H	10.13568300	-1.58167100	-1.84367400
H	11.58366500	0.05544100	-0.65695900
H	10.55354500	1.75863600	0.83405000
H	8.10952700	1.81478200	1.15164000
H	5.96357600	-1.93849300	-0.03895000
H	3.72163600	2.46811800	0.38628000
H	6.11949500	2.35040800	0.07273400
H	3.78689700	-3.08580800	0.16190800
H	1.32711400	-2.93650400	0.33186200
H	-0.58002900	-1.78102900	0.69934000
H	-0.62074100	1.08914900	-0.38849200

H	-2.63466500	1.98248300	-1.09461100
H	-5.03513700	1.94360900	-1.31824800
H	-5.12299400	-1.89444000	0.70732700
H	-2.73634800	-1.84611100	0.89605600
H	-6.89648400	2.07177900	-0.74295600
H	-7.67249600	1.03544100	-1.96255200
H	-8.56154200	1.57949400	0.92546100
H	-9.36494900	2.09731900	-0.57321500
H	-9.37471700	-1.96565400	0.31448600
H	-8.56657200	-0.87494500	1.46405800
H	-7.71576800	-1.51200800	-1.41417900
H	-6.91148200	-2.04166000	0.06899400
H	-11.43100100	-0.73970500	0.31225900
H	-11.42981800	0.98863300	-0.07935700
H	-10.82350000	0.43890300	1.50497800
H	2.12879400	2.06323600	1.75704400
H	1.28204000	2.31013900	0.20921700
H	0.50274600	1.39955900	1.52993300

References

1. K. Qiu, Y. Chen, T. W. Rees, L. Ji and H. Chao, *Coord. Chem. Rev.*, 2019, **378**, 66-86.
2. B. Chen, C. Li, J. Zhang, J. Kan, T. Jiang, J. Zhou and H. Ma, *Chem. Commun.*, 2019, **55**, 7410-7413.
3. Y. Song, H. Zhang, X. Wang, X. Geng, Y. Sun, J. Liu and Z. Li, *Anal. Chem.*, 2021, **93**, 1786-1791.
4. C. Lee, W. Yang and R. G. Parr, *Phys. Rev. B*, 1988, **37**, 785-789.
5. A. D. Becke, *J. Chem. Phys.*, 1992, **96**, 2155-2160.
6. A. D. Becke, *Phys. Rev. A*, 1988, **38**, 3098-3100.
7. W. J. Hehre, *Acc. Chem. Res.*, 1976, **9**, 399-406.
8. N. M. O'Boyle, A. L. Tenderholt and K. M. Langner, *J. Comput. Chem.*, 2008, **29**, 839-845.
9. W. Humphrey, A. Dalke and K. Schulten, *J. Mol. Graph.*, 1996, **14**, 33-38.
10. O. Trott and A. J. Olson, *J. Comput. Chem.*, 2010, **31**, 455-461.
11. T. A. Larsen, D. S. Goodsell, D. Cascio, K. Grzeskowiak and R. E. Dickerson, *J. Biomol. Struct. Dyn.*, 1989, **7**, 477-491.